Geobiology (2006), **4**, 271–283 DOI: 10.1111/j.1472-4669.2006.00085.x

The loss of mass-independent fractionation in sulfur due to a Palaeoproterozoic collapse of atmospheric methane

K. ZAHNLE,[1] M. CLAIRE[2] AND D. CATLING[2,3]

[1]*NASA Ames Research Center, MS 245-3, Moffett Field, CA 94035, USA*
[2]*Astrobiology Program and Department of Atmospheric Sciences, Box 351640, University of Washington, Seattle, WA 98195-1640, USA*
[3]*Department of Earth Sciences, University of Bristol, Wills Memorial Building, Queen's Road, Bristol BS8 1RJ, UK*

ABSTRACT

We use a 1-D numerical model to study the atmospheric photochemistry of oxygen, methane, and sulfur after the advent of oxygenic photosynthesis. We assume that mass-independent fractionation (MIF) of sulfur isotopes – characteristic of the Archean – was best preserved in sediments when insoluble elemental sulfur (S_8) was an important product of atmospheric photochemistry. Efficient S_8 production requires three things: (i) very low levels of tropospheric O_2; (ii) a source of sulfur gases to the atmosphere at least as large as the volcanic SO_2 source today; and (iii) a sufficiently high abundance of methane or other reduced gas. All three requirements must be met. We suggest that the disappearance of a strong MIF sulfur signature at the beginning of the Proterozoic is better explained by the collapse of atmospheric methane, rather than by a failure of volcanism or the rise of oxygen. The photochemical models are consistent in demanding that methane decline before O_2 can rise (although they are silent as to how quickly), and the collapse of a methane greenhouse effect is consistent with the onset of major ice ages immediately following the disappearance of MIF sulfur. We attribute the decline of methane to the growth of the oceanic sulfate pool as indicated by the widening envelope of mass-dependent sulfur fractionation through the Archean. We find that a given level of biological forcing can support either oxic or anoxic atmospheres, and that the transition between the anoxic state and the oxic state is inhibited by high levels of atmospheric methane. Transition from an oxygen-poor to an oxygen-rich atmosphere occurs most easily when methane levels are low, which suggests that the collapse of methane not only caused the end of MIF S and major ice ages, but it may also have enabled the rise of O_2. In this story the early Proterozoic ice ages were ended by the establishment of a stable oxic atmosphere, which protected a renewed methane greenhouse with an ozone shield.

Received 14 June 2006; accepted 11 August 2006

Corresponding author: K. Zahnle. Tel.: 650 604 0840; fax: 650 604 6779; e-mail kevin.j.zahnle@nasa.gov.

INTRODUCTION

Mass-independent fractionation (MIF, or nonzero $\Delta^{33}S$) of stable sulfur isotopes is widely recognized as a defining geological signature of the Archean Earth, even though the origin of the signal remains somewhat obscure. What is striking about the isotopic signature is that (i) it exists at all; (ii) the signal is strong through much of the Archean; and (iii) the strong signal seems to disappear abruptly ca. 2.45 Ga (Farquhar *et al.*, 2000; Farquhar & Wing, 2003; Bekker *et al.*, 2004; Papineau *et al.*, 2005), just before a set of severe ice ages began, and somewhat before the classic indicators of an anoxic atmosphere disappeared and the classic indicators of an oxic atmosphere appeared (Cloud, 1968, 1988; Walker, 1977; Walker *et al.*, 1983; Kasting, 1993; Holland, 1999, 2002; Canfield, 2005; Catling & Claire, 2005). A much weaker MIF signal lingered on for some 400 Myr (Farquhar *et al.*, 2003; who call the middle interval Stage 2), but clearly something changed abruptly and permanently.

Leading interpretations of the end of MIF stress the rise of O_2 as the cause (Farquhar *et al.*, 2000; Pavlov & Kasting, 2002; Ono *et al.*, 2003). These arguments are based on considerations of atmospheric photochemistry that will be discussed in detail below. The earlier consensus had placed the rise of O_2 at 2.2 or 2.3 Ga (cf. Holland, 1999, 2002), some 200 Myr after MIF S disappeared. The old chronology was strongly

influenced by a pronounced and long-lasting excursion in carbonate $\delta^{13}C$ values between 2.05 and 2.25 Ga (Des Marais *et al.*, 1992; Karhu & Holland, 1996). The isotope excursion has been widely interpreted as a major carbon burial event that in some sense caused the rise of O_2 (Karhu & Holland, 1996). Whether there truly was a 200 Myr delay between the end of Stage 1 and the advent of an oxic atmosphere seems debatable, because the dates are uncertain and because the sedimentary record has been compromised by the ice ages (Farquhar & Wing, 2005). Nevertheless, the apparent mismatch between the two chronologies raises questions about why MIF S stopped when it did.

Known mechanisms for generating MIF signals require gas phase photochemistry stemming from the ultraviolet (UV) photolysis of SO_2 (Farquhar *et al.*, 2001). Laboratory experiments show that SO_2 photolysis at 193 nm generates a strong MIF signal in the photolysis products and that 248 nm does not (Farquhar *et al.*, 2000). Farquhar *et al.* (2001) hypothesized that the major source of the MIF signal is the photodissociation of SO_2 to SO and O, a channel that cuts off at 220 nm. More recent laboratory work suggests that MIF S can occur at wavelengths somewhat longer than 220 nm through excited states of SO_2 (Masterson *et al.*, 2006).

In an oxic atmosphere, photons longer than 200 nm are chiefly absorbed by ozone. However, ozone is not extremely opaque to $200 < \lambda < 220$ nm; this is a spectral window between much stronger absorption at shorter wavelengths by water and CO_2 and at longer wavelengths by ozone. Consequently, it requires a considerable column of ozone, approaching modern levels, to fully suppress MIF-generating SO_2 photolysis. This in turn requires a considerable amount of O_2, on the order of 0.01 PAL (Kasting & Donahue, 1980; PAL means Present Atmospheric Level). We therefore would expect MIF S to persist in atmospheric gases until the atmosphere became mildly aerobic (Farquhar & Wing, 2005). Even today nonzero $\Delta^{33}S$ is found in some Antarctic ices, where it derives from stratospheric photochemical processing of volcanic gases and where competition from other sulfur sources is small (Savarino *et al.*, 2003).

In the discovery paper, Farquhar *et al.* (2000) pointed out that the observed sedimentary signature of MIF S is best explained by separating the photochemically processed sulfur into water-soluble and water-insoluble fractions. Separate soluble and insoluble channels have the additional advantage of discouraging the sulfur from pooling in the oceans, where the various S-containing species would mix back together and the MIF signature would be diluted or lost (Pavlov & Kasting, 2002). Pavlov & Kasting (2002) suggested that the key vector was elemental sulfur (S_8), which is insoluble and which photochemical modelling indicates a major product of sulfur photochemistry in oxygen-poor atmospheres (Kasting *et al.*, 1989). Pavlov & Kasting (2002) computed that O_2 levels as low as 10^{-5} PAL (2 ppmv) would shut off S_8 production and thus prevent MIF S from reaching the sediments.

A potential problem with Pavlov & Kasting's (2002) result is that their model was not capable of treating atmospheres with intermediate levels of oxygen. Instead they used separate photochemical models for high and low oxygen levels. The two models do not meet in the middle. Unfortunately it is precisely in this unexplored space in the middle that S_8 production shuts off. We have therefore decided to revisit the S_8 production threshold using a model that does not have this problem.

In this study we accept the hypothesis that MIF S records the precipitation of S_8 from the atmosphere. However, we will show that S_8 production shuts off well before the atmosphere becomes oxic. In keeping with our focus on the rise of oxygen, we restrict our discussion to Earth after the origin of oxygenic photosynthesis.

THE PHOTOCHEMICAL MODEL

For our numerical experiments we used an updated version of the 1-D diffusive photochemical code originally developed by Kasting *et al.* (1989) to study sulfur photochemistry on early Earth. The version used here includes 46 chemical species that participate in 206 chemical reactions. As we will consider only atmospheres with more CO_2 than CH_4, hazes do not form (Zahnle, 1986), and so we truncate hydrocarbon chemistry at C_2H_6. Vertical transport occurs by eddy transport. H_2 and H also flow upward by molecular diffusion. The equations solved are

$$N\frac{\partial f_i}{\partial t} = P_i - L_i N f_i - \frac{\partial \phi_i}{\partial z} \qquad (1)$$

and

$$\phi_i = b_{ia} f_i (H_a^{-1} - H_i^{-1}) - (b_{ia} + KN)\frac{\partial f_i}{\partial z} \qquad (2)$$

where N is the atmospheric density; f_i is the mixing ratio of the (minor) species i; $P_i - L_i N f_i$ are the chemical production and loss terms, respectively; ϕ_i is the upward flux of species i; b_{ia} is the binary diffusion coefficient between i and the background atmosphere a; H_a and H_i are the scale heights of the background atmosphere and of species i; and K is the eddy diffusion coefficient.

General model assumptions

Steady-state solutions are obtained for an average sun angle of 50°. The surface temperature is set to 284 K, the tropopause is at $z_{tr} = 11$ km, and the stratosphere is isothermal at 186 K. Tropospheric water vapor follows the Manabe-Wetherald (1967) relative humidity profile. The eddy diffusivity is set to 10^5 cm^2 s^{-1} in the troposphere and to $10^3(p(z_{tr})/p(z))^{0.5}$ cm^2 s^{-1} in the stratosphere. To take some account of the higher activity of the Sun ca. 2.5 Ga, UV at wavelengths longer than 175 nm is doubled over today and UV at wavelengths shorter than

175 nm is quadrupled (Ribas *et al.*, 2005). The surface pressure is set to 1 bar of N_2. The CO_2 mixing ratio is set at 1%. The top of the model is at 80 km. Results are not very sensitive to any of these assumptions.

Sulfur chemistry

Sulfur is injected into the atmosphere abiogenically as volcanic gases, chiefly SO_2 and H_2S, and it enters the atmosphere biogenically chiefly as CH_3SCH_3 (dimethyl sulphide, usually written 'DMS'), OCS, and CS_2 (Toon *et al.*, 1987). Our model does not yet include CS_2, DMS and their photochemical products. These gases are important when the biogenic sulfur source is strong, as seems likely for the late Archean and early Proterozoic. DMS in particular is thought to be produced exclusively by eukaryotic phytoplankton (Charlson *et al.*, 1987). A more complete accounting of the sulfur cycle that takes biogenic sources into account is clearly desirable but fell beyond the scope of this study.

In today's oxic atmosphere, S is either rained out as SO_2 or it is oxidized to SO_3, which after prompt reaction with H_2O precipitates as sulfuric acid (H_2SO_4). In a more reduced ancient atmosphere, sulfur can take any oxidation state from –2 to +6 (Kasting *et al.*, 1989). As today, S can exit the atmosphere as SO_2 or H_2SO_4, but there are more reduced options as well. Most S-containing species are moderately soluble (SO_2, H_2S, OCS, CS_2) and can be washed out of the atmosphere in rain. If the atmosphere is sufficiently reducing and the sulfur source big enough, elemental sulfur particles can form and precipitate (Kasting *et al.*, 1989; Pavlov & Kasting, 2002; Ono *et al.*, 2003).

The model includes rainout of soluble species in proportion to their presence in raindrops. The model also includes sulfuric acid aerosols and elemental sulfur particles. H_2SO_4 condenses when its saturation vapor pressure is exceeded; the H_2O/H_2SO_4 ratio of the particles is self-consistently predicted. Elemental sulfur particles can form when photochemically produced HS and S combine to form S_2. The S_2 can polymerize to form longer chains (the model uses only S_3 and S_4). Polymerization is assumed to stop at the stable ring molecule S_8, which is then assumed to immediately condense. Kasting *et al.* (1989), Kasting (1990), and Pavlov *et al.* (2001) describe in more detail how rainout, aerosol formation and deposition are implemented.

Redox

The model cannot explicitly conserve H or O because tropospheric water vapor is set by evaporation and precipitation of what is in effect an infinite ocean of water. However, the difference between H_2 and O – the redox – is conserved, and it is imperative that it be conserved in a model that purports to compute the redox state of the atmosphere.

It is convenient to define H_2O, N_2, CO_2, and SO_2 as the redox neutral gases. These are the most important volcanic gases for H, N, C, and S, respectively. The redox state of the atmosphere can be defined as the number of extra O atoms minus half the number of extra H atoms. For example, with this definition, H_2SO_4 has a redox state of +1 ($H_2SO_4 = H_2O + SO_2 + O$), and HCO has a redox state of –1.5 ($HCO = CO_2 + \frac{1}{2} H_2O - \frac{3}{2} O$). Minor volcanic gases, such as CO, H_2, and H_2S, are reducing. By assumption the major biogenic gases are CH_4 and O_2, the former strongly reducing and the latter strongly oxidizing. Other important terms in the atmosphere's redox budget include precipitation of S_8 and H_2SO_4 aerosols; rainout of soluble species, especially H_2CO and H_2O_2; and hydrogen escape to space.

Redox conservation is one of the best tests of how credibly the photochemical code performs and consequently it has been the focus of a great deal of development effort. The photochemical code used here always maintains redox conservation to better than 10 ppb, and usually to better than 10 ppt, when the O_2 source is significant. This is excellent performance. The code does not perform as well when the O_2 source is negligible, as would have been the case before the advent of oxygenic photosynthesis. In this study we use the code only in regimes in which it performs extremely well.

Hydrogen escape

We treat hydrogen escape using diffusion-limited flux. Diffusion-limited escape makes the single assumption that escape is easy for hydrogen once it has diffused through the lower, well-mixed atmosphere. This is a good approximation for Earth today. The upper boundary condition is implemented by setting an escape velocity at the top of the computational grid. In diffusion-limited flux the effusion velocity at the top of the grid is

$$v_e = \frac{b_{ia}}{N}(H_a^{-1} - H_i^{-1}). \quad (3)$$

Equation 3 is readily derived from Equation 2 in the limit that $\partial f/\partial z \to 0$ (e.g. Walker, 1977). In diffusion-limited escape with modern volcanic degassing fluxes and no biology, the H_2 mixing ratio would be on the order of 100–1000 ppmv, depending on the exuberance of the volcanic flux.

It has recently been suggested that the hydrogen escape rate might have been much lower than the diffusion-limited flux (Tian *et al.*, 2005). The Tian *et al.* (2005) model makes several assumptions that suppress H escape, the most important of which is to assume that the thermosphere was cold. The motivation for their model is that the thermospheres of Venus and Mars – both of which have CO_2 atmospheres – are cool. In our opinion Tian *et al.* (2005) have not made a convincing case against diffusion-limited flux for Earth (Catling, 2006).

Lower boundary conditions

Minor gases are treated assuming deposition velocities (in many cases set to zero, but these do not matter much because

Table 1 Volcanic fluxes. All quantities given in units of molecules cm^{-2} s^{-1}

Model title	SO_2	H_2S	H_2	CO
V1 – 'modern low'	1×10^9	1×10^8	2×10^9	2×10^8
V2 – 'modern high'	3.5×10^9	3.5×10^8	1×10^{10}	1×10^9
V3 – 'Archean high'	1×10^{10}	1×10^9	3×10^{10}	3×10^9

they are minor). The important lower boundary conditions are those for which the lower boundary is (or can be) an important source. In our model these species are O_2, CH_4, H_2, CO, SO_2, and H_2S. For most of the numerical experiments discussed in this study we have used constant mixing ratio boundary conditions for CH_4 and O_2, and constant flux boundary conditions for important volcanic gases H_2S, H_2, and CO. Kasting *et al.* (1989) argued that dissolution of SO_2 into the ocean was a major sink for SO_2. To allow for surface deposition of SO_2, we distributed the volcanic SO_2 source over the troposphere and lower stratosphere; this is also more in keeping with the nature of volcanic eruptions. Numerical experiments using flux boundary conditions on CH_4 and O_2 provide a different perspective on the relative likelihood of different atmospheres, but as a practical matter constant mixing ratio boundary conditions are computationally more robust and better suited to generating suites of output.

We also consider two alternative sets of lower boundary conditions on H_2 and CO. One set is simply to impose low mixing ratios at the surface (10 ppmv for H_2 and 1 ppmv for CO) that implicitly presume voracious biological consumption. A second set is to impose deposition velocities at the surface that take into account the rate that gases can cross the air–water interface. Kharecha *et al.* (2005) suggest $v_{dep} = 2.5 \times 10^{-4}$ cm s^{-1} for H_2 and $v_{dep} = 1.2 \times 10^{-4}$ cm s^{-1} for CO. To include either of these alternatives as LBCs requires distributing the volcanic source. We distribute that source in the same way that we distribute volcanic SO_2. Numerical experiments indicate that model results are insensitive to the lower boundary conditions on H_2 and CO save where the biogenic O_2 and CH_4 sources are small.

Volcanic sources

We consider three sets of volcanic fluxes, which we call 'low modern', 'high modern', and 'high Archean'. We denote these cases V1, V2, and V3, respectively. These cases are summarized in Table 1. In practice the important role of volcanic gases in these simulations is that they are the source of S-containing gases to the atmosphere. The role of volcanic gases in governing the redox state of the atmosphere – crucial to dead planets – is questionable on a living world, and as a practical matter our numerical simulations are not very sensitive to CO and H_2 volcanic fluxes.

For H_2 we use a low modern flux of 2×10^9 cm^{-2} s^{-1} ($= 5 \times 10^{11}$ mol $year^{-1}$), as recommended by Sleep & Bird (2006). This estimate includes arc volcanoes and a serpentinization source of the same magnitude. The arc flux is based on the rate that hydrous minerals in ocean basalts are subducted and a volcanic QFM H_2/H_2O ratio of 0.02. Pavlov & Kasting (2002) used a much higher H_2 flux of 2.5×10^{10} cm^{-2} s^{-1} for the Archean, which they attribute to Holland (1984). Holland's most recent estimate for $\phi(H_2)$ is 1.8×10^{10} cm^{-2} s^{-1} (Holland, 2002). Holland's estimate is bigger than Sleep and Bird's (2006) because Holland uses a bigger volcanic flux of H_2O, which he obtains from the CO_2 outgassing flux using a reported CO_2/H_2O ratio of 0.03. We have used 1×10^{10} cm^{-2} s^{-1} as the high modern flux for H_2.

For CO we scale directly from the reported modern volcanic CO_2 source of 3×10^{10} cm^{-2} s^{-1} (Sleep & Zahnle, 2001; Zahnle & Sleep, 2002) using a volcanic QFM CO/CO_2 ratio of 0.03. This results in a volcanic CO flux of 8×10^8 cm^{-2} s^{-1}. We use 2×10^8 cm^{-2} s^{-1} for a low modern case and 1×10^9 cm^{-2} s^{-1} for the high modern case.

Walker & Brimblecombe (1985) presented strong arguments that oceanic sulfate in the Archean had as its main source volcanic gases, chiefly SO_2 and H_2S. Estimates of the modern SO_2 range between 1×10^9 and 3×10^9 cm^{-2} s^{-1} (Andres & Kasgnoc, 1998; Marty & Tolstikhin, 1998; Arthur, 2000). We use 1×10^9 for the low modern value and 3.5×10^9 as the high modern value, as the latter is the SO_2 outgassing rate used by Pavlov & Kasting (2002). Ono *et al.* (2003) consider 3.5×10^8, 1×10^9, and 3.5×10^9 cm^{-2} s^{-1} for their low, medium and high volcanic fluxes, respectively.

The H_2S/SO_2 ratio is more uncertain. The volcanic QFM ratio of 0.02 is lower than field measurements seem to indicate. Recent measurements imply that the ratio can be much higher in certain volcanoes (Aiuppa *et al.*, 2005). Global estimates for H_2S flux range from 2×10^8 and 7.7×10^9 cm^{-2} s^{-1}. Given the uncertainty, we have arbitrarily fixed the H_2S/SO_2 at 0.1 for all three cases.

We assume that Archean volcanic fluxes were roughly three times higher than modern volcanic fluxes. Hence for V3, we use 3×10^{10}, 3×10^9, 1×10^{10}, and 1×10^9 cm^{-2} s^{-1} for H_2, CO, SO_2, and H_2S, respectively.

Oxygen and methane

There is compelling evidence preserved in molecular fossils that oxygenic photosynthesis originated no later than 2.75 Ga (Brocks *et al.*, 1999, 2003; Summons *et al.*, 2006) and therefore at least 300 Myr before the end of MIF S and 500 Myr before the rise of O_2. Early consequences of oxygenic photosynthesis are a jump in primary productivity and a jump in atmospheric methane (Walker, 1987; Catling *et al.*, 2001; Claire *et al.*, 2006). We expect the latter for two reasons. First, with more organic matter to ferment, more fermentation is to be expected; and second, because O_2 is a much more reactive molecule than CH_4, we expect that the geochemical sink for O_2 would have been bigger than the sink on CH_4 until the

crust was oxidized. By contrast Kopp *et al.* (2005) reject a lengthy delay between the advent of oxygenic photosynthesis and the appearance of abundant free O_2. They suggest instead that oxygenic photosynthesis was invented during the early Proterozoic ice ages ca. 2.3 Ga and promptly annihilated a pre-existing methane greenhouse.

A fundamental assumption underlying most of our numerical experiments is that the net flux of photosynthetic O_2 into the atmosphere was approximately stochiometrically balanced by the net flux of biogenic reduced gases into the atmosphere, chiefly CH_4. The justification for this is that the atmosphere is a small reservoir that quickly equilibrates with the chemical forcing. The balance is inexact because we do not force it explicitly – our explicit assumption is that an atmosphere can exist with the ground level O_2 and CH_4 mixing ratios we prescribe. The photochemical model does the accounting and computes the fluxes consistent with a photochemical steady state. Any stochiometric imbalance between CH_4 and O_2 is accounted for in several generally smaller terms in the atmospheric redox budget, including H escape, rainout of reduced and oxidized species, volcanic gases, and fallout of sulfur.

By conserving the redox budget of the atmosphere, we have in effect put a bag around the atmosphere. The redox fluxes of gases entering and exiting the bag sum to zero. So far as the atmosphere is concerned, this is correct: our possible atmospheres are self-consistent. We have not attempted to apply redox balance to the oceans, sediments, crust, and mantle that lie outside the bag. In our model there is in general a small net difference between the reducing power of volcanic gases added to the atmosphere and the reducing power lost to the atmosphere by hydrogen escape. This difference is proximally added to (or extracted from) the oceans. There are many terms in the ocean's redox budget that are comparable to or bigger than the atmospheric term. These include burial of reduced carbon in sediments, subduction of sediments and altered oceanic crust, volcanic gases vented directly into the oceans, and reduced or oxidized sediments and altered crust accreted by or weathered from continents. These terms involve big reservoirs with long time constants (e.g. 100 Myr for reduced carbon in continental sediments) that are not plausibly held to redox balance on time scales relevant to the atmosphere.

Captive cyanobacterial mats grown and monitored in the laboratory emit O_2 in the day and H_2 at night (Hoehler *et al.*, 2001). The mats do not emit much CH_4 because methanogens lose the competition with sulfate reducers, and in the mats sulfate is generally present in excess. A net excess of photosynthetic O_2 is balanced not by burial of organic carbon but rather by the loss, or export of, soluble organic matter to the waters beyond the mat. The exported oceanic organic matter can be oxidized with sulfate and, if the sulfate runs out, it can be biologically reduced to CH_4.

Hydrogen has similar photochemical effects to CH_4 in an anoxic atmosphere with an underlying photosynthetic source of O_2. In particular, it is comparably effective as a reducing agent to precipitate S_8. If other factors are neglected, a big biogenic H_2 source provides as good an explanation for MIF S as a big biogenic source of CH_4. In other words MIF S does not distinguish between H_2 and CH_4 as the reduced partner to photosynthetic O_2.

Of course other factors do matter. One difference is that methane is not as biologically desirable as hydrogen. Methane can be eaten aerobically or anaerobically using sulfate (Valentine, 2002). In the anoxic atmosphere aerobic oxidation would be restricted to localized oases. Sulfate would have been relatively unimportant while oceanic sulfate was scarce, as it was through much of the Archean (Canfield *et al.*, 2000; Canfield, 2005). Anaerobic methane oxidation using sulfate provides another reason to expect that the methane source shrank as oceanic sulfate grew. On the other hand H_2 is very useful biologically for many purposes. We expect that the biological sink on atmospheric H_2 has always been significant. Some of the H_2 is converted to CH_4 by ordinary methanogenesis. A second difference is that CH_4 is an effective greenhouse gas; much of what makes methane attractive to theorists is that it is the only plausible supplement to CO_2 as a way of keeping the young Earth warm (Pavlov *et al.*, 2000).

RESULTS

Our numerical experiments are performed over a grid of constant O_2 and CH_4 ground-level mixing ratios. For CH_4 we consider mixing ratios between 10^{-6} and 10^{-3}. For O_2 we consider a wider range of mixing ratios, from extremely anoxic cases with less than 10^{-14} to quasi-modern atmospheres with 10^{-2}.

O_2 and CH_4 are photochemically consumed in the atmosphere to make CO_2 and H_2O. In the model, O_2 and CH_4 flow in through the lower boundary to maintain the assumed constant ground-level mixing ratios; this inflow we identify with the biogenic sources. When the model reaches steady state the computed O_2 and CH_4 lower boundary fluxes exactly balance the net photochemical destruction.

Long-lived CH_4 is generally well mixed, but O_2 is only well mixed when it is more abundant than methane. Examples of oxic and anoxic atmospheres are shown in Figs 1 and 2. To first approximation the less oxic atmospheres feature oxic stratospheres but extremely anoxic tropospheres. In these atmospheres, oxygen mixes up from the surface photosynthetic source and it mixes down from the stratosphere, to be consumed by the troposphere in the middle. This is a general property of reduced atmospheres.

Sulfate aerosols are produced at all heights, especially in the relatively oxidizing stratosphere. Elemental sulfur aerosols tend to form in the anoxic troposphere or near the tropopause, where descending products of SO_2 photolysis mix with ascending reduced gases from the troposphere. Figures 3 and 4 show where sulfur and sulfate aerosols form in the oxic and anoxic atmospheres of Figs 1 and 2. These are for the high

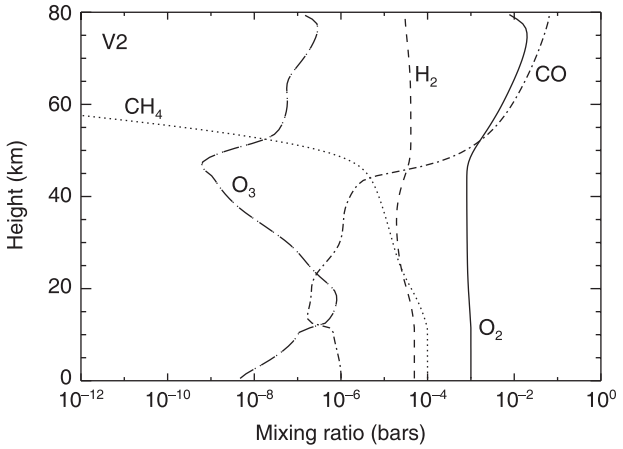

Fig. 1 Mixing ratios of some important atmospheric gases as a function of altitude for an example oxic atmosphere. This model assumes ground-level mixing ratios $f(O_2) = 10^{-3}$ and $f(CH_4) = 10^{-3}$. Volcanic fluxes Model V2. Note that O_2 and CH_4 are both reasonably well-mixed below 50 km.

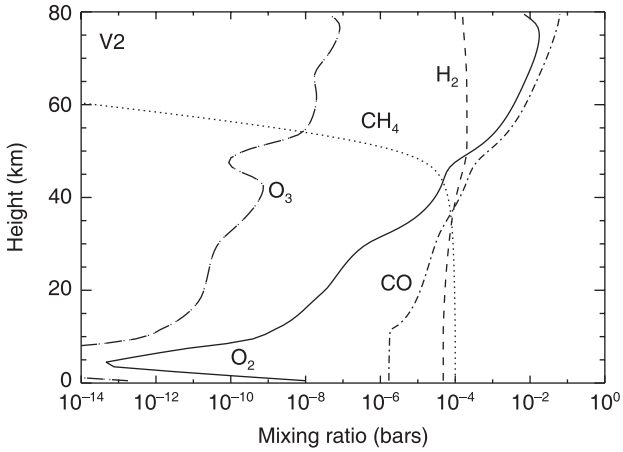

Fig. 2 Mixing ratios of some important atmospheric gases as a function of altitude for an example anoxic atmosphere. This model assumes ground-level $f(O_2) = 10^{-8}$ and $f(CH_4) = 10^{-3}$. Volcanic fluxes Model V2. Note that O_2 is drastically ill-mixed, and that the troposphere is extremely anoxic despite the surface being a strong source of photosynthetic O_2.

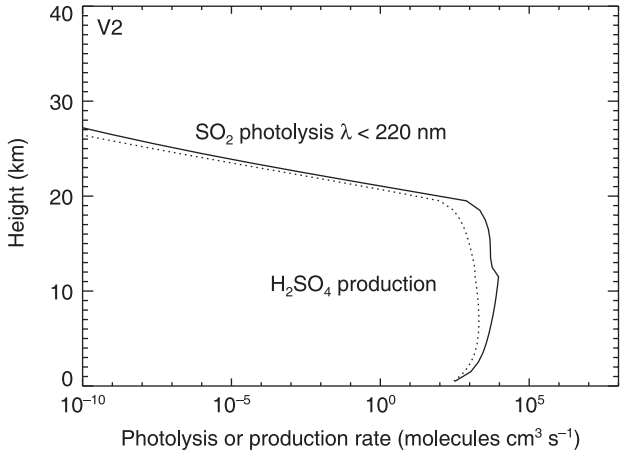

Fig. 3 Altitudes of sulfate and sulfur aerosol production compared to the altitudes where SO_2 absorbs UV shorter than 220 nm in an oxic atmosphere with $f(O_2) = 10^{-3}$ and $f(CH_4) = 10^{-4}$ and $\phi(SO_2) = 3.5 \times 10^9$ cm^{-2} s^{-1} (V2). SO_2 rainout (not shown) is a major loss process but is confined to the troposphere ($z < 11$ km). The near coincidence of the SO_2 photolysis rate and the H_2SO_4 formation rate is accidental.

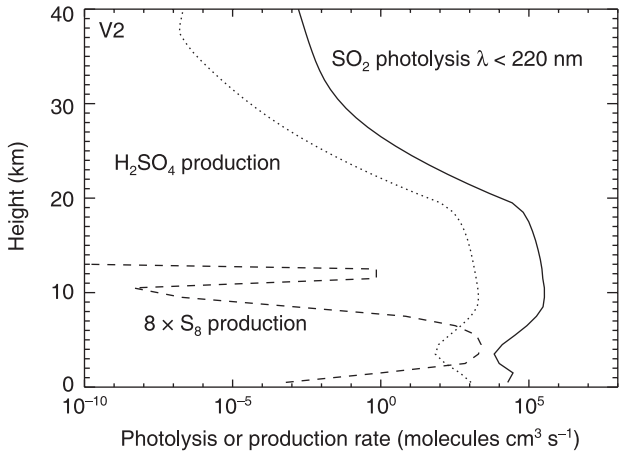

Fig. 4 Altitudes of sulfate and sulfur aerosol production compared to the altitudes where SO_2 absorbs UV shorter than 220 nm in a moderately anoxic atmosphere with $f(O_2) = 10^{-8}$ and $f(CH_4) = 10^{-4}$ and $\phi(SO_2) = 3.5 \times 10^9$ cm^{-2} s^{-1} (V2). We expect the MIF S signal to be strongest when the production regions of S_8 and sulfate overlap with the region where SO_2 absorbs UV shorter than 220 nm. These conditions are met in this model. Elemental sulfur forms mostly in or near the strongly reduced troposphere, while sulfate forms everywhere. A more deeply anoxic atmosphere would suppress sulfuric acid formation in the troposphere.

modern volcanic S fluxes (V2). The S_8 and H_2SO_4 formation regions are compared to where SO_2 absorbs UV shorter than 220 nm. Rainout of SO_2, which is not shown, is confined to the troposphere. We expect that the MIF S signal is strongest when the production regions of S_8 and sulfate overlap with the region where SO_2 absorbs $\lambda < 220$ nm. These conditions are met in all the anoxic models.

In each model with significant S_8 deposition, we verified that the SO_2 photolysis rate by the MIF-producing photons ($190 < \lambda < 220$ nm, for $SO_2 + h\nu \rightarrow SO + O$) was higher than the S_8 production rate at every height at which S_8 was produced. In addition, each model shows numerically higher S production rates by the photolysis of $SO + h\nu \rightarrow S + O$, along with higher total S, S_2 and S_4 production rates at each model altitude with S_8 production. We use the above tests to identify our deposited S_8 as a likely carrier of the MIF signal, given that Pavlov & Kasting (2002) have shown that the MIF signature is distributed among sulfur species in an anoxic atmosphere.

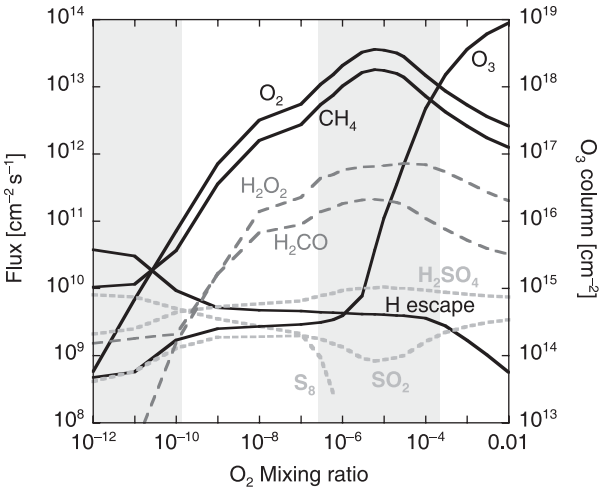

Fig. 5 Major fluxes as a function of O_2 mixing ratio ($f(O_2)$) for a CH_4 mixing ratio fixed at 100 ppmv; the ozone column is shown against the right-hand axis. The CH_4 and O_2 fluxes are net biogenic sources. For the most part, O_2 and CH_4 in the atmosphere mutually annihilate. Hydrogen peroxide is the most important oxidized product, and formaldehyde is the most important reduced product; both rain out and their fluxes are shown. Hydrogen escape is most important at low $f(O_2)$ and becomes less important as $f(O_2)$ increases. Decreasing O_2 and CH_4 fluxes at high $f(O_2)$ is caused by the increasingly effective ozone shield. The shaded regions represent cases where the net biogenic O_2 fluxes are either implausibly low ($<10^{11}$) or implausibly high ($>10^{13}$ cm^{-2} s^{-1}). At 100 ppmv methane, plausible atmospheres can be oxic or anoxic yet generated by effectively the same biological forcing. Either state is allowable, although the states in between are not. Only the anoxic solution generates S_8. Transition between the oxic and anoxic states is precluded by the impossibly high O_2 fluxes required; transition requires lowering CH_4 levels significantly below 100 ppmv. These are for the high Archean volcanic flux (V3).

Figure 5 is a summary figure over a grid of models differing only in the prescribed ground-level O_2 mixing ratio. The CH_4 mixing ratio is fixed at 100 ppmv, which is near the lower limit of what would be required for methane greenhouse warming to maintain temperate conditions at Earth's surface 2.8 Ga, given the upper limit on atmospheric CO_2 inferred by Rye *et al.* (1995). Figure 5 treats the O_2 mixing ratio as the independent variable. This gives an accurate description of how the photochemical model was implemented. The dependent variables are the O_2 and CH_4 fluxes required to sustain the assumed mixing ratios, and the various fluxes of chemical products leaving the atmosphere. The most important of the latter are rainout of formaldehyde (H_2CO) and hydrogen peroxide (H_2O_2).

Perhaps the first thing one sees in Fig. 5 is that the O_2 and CH_4 fluxes peak at an O_2 mixing ratio of 10 ppmv. The peak is caused by rising levels of ozone (also shown against the right hand axis). At low O_2 mixing ratios ozone is unimportant and the photochemical reactions between CH_4 (and its products) and O_2 (and its products) increase as O_2 increases. But at higher O_2 levels the ozone becomes abundant enough that a significant fraction of the incident UV photons are wasted shuttling oxygen atoms between O_2 and O_3: $O_2 + O \rightarrow O_3$, $O_3 + h\nu \rightarrow O_2 + O$. In atmospheric photochemistry the ultimate speed limit is set by the number of photons.

As a philosophical point, one thinks of the O_2 and CH_4 fluxes as the true independent variables, and of the O_2 and CH_4 mixing ratios as the consequences of photochemical reactions acting upon the fluxes. This is correct to the extent that the effect of mixing ratios upon biological activity can be ignored – a significant caveat. When Fig. 5 is viewed from the perspective of flux as the independent variable, one sees that the solution is multiple valued. The same level of biological productivity can support either a highly anoxic or a rather oxic atmosphere. There is something to this, but recall that we have fixed CH_4 at 100 ppmv; as depicted here, the demonstration of multiple solutions is rigorously valid only if there is an external control over $f(CH_4)$, as for example might be provided by a Gaian thermostat.

Another perspective on Fig. 5 is to view the increase in $f(O_2)$ as an evolution through time. This is tempting; after all, O_2 did increase. Again there is something to this, but again, one must not ascribe too much import to $f(O_2)$ as an independent variable; it is not. Rather, explaining why $f(O_2)$ increases (i.e. the quest for the true independent variable) drives this whole field of research. An additional complication in viewing Fig. 5 as an evolutionary plot is that methane levels do not remain constant and are likely anticorrelated to oxygen levels in a nonlinear fashion (Claire *et al.*, 2006).

Figure 5 also shows the three major losses for atmospheric sulfur. Fallout of sulfuric acid particles and rainout of SO_2 occur at all $f(O_2)$ but fallout of S_8 is restricted to anoxic atmospheres with $f(O_2) < 10^{-6}$. Separate exits through sulfate or through SO_2 allow for some preservation of photochemical MIF S in more oxic atmospheres, but as noted above the signal would be diluted or lost when the species dissolved together in liquid water. Today MIF S is restricted to extremely dry environments. In the early Proterozoic the MIF signal in SO_2 and sulfate should have been stronger, while the ozone layer was thinner and lower; perhaps there is some explanation here for Stage II as defined by Farquhar *et al.* (2003).

The O_2 and CH_4 fluxes in Fig. 5 are large. The modern gross CH_4 flux is 1.5×10^{12} cm^{-2} s^{-1}. About 90% of this is consumed by methanotrophs before it reaches the atmosphere; we presume that a much higher fraction reached the anoxic atmosphere.

In the modern world oxygenic photosynthesis generates O_2 at a rate of $\sim 4 \times 10^{13}$ cm^{-2} s^{-1} (Walker, 1977). Obviously most of this O_2 is respired. Today, on geological time scales the net O_2 flux into the atmosphere is balanced by oxidation of rocks, minerals, and fossil carbon at a rate on the order of $\sim 4 \times 10^{10}$ cm^{-2} s^{-1} (Holland, 1984). On shorter time scales the imbalances are bigger. The annual imbalance between photosynthesis and respiration can be seen in the 6 ppmv annual variation of atmospheric CO_2, which implies that on

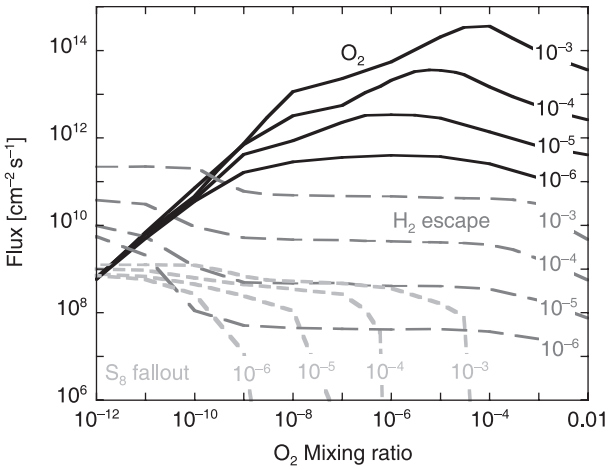

Fig. 6 O_2 flux, H escape, and S_8 fallout as a function of $f(O_2)$ for $f(CH_4)$ between 10^{-6} and 10^{-3}. Curves are labelled by $f(CH_4)$. Hydrogen escape and the threshold for S_8 production increase directly with the amount of CH_4 in the atmosphere. Note that transition between low and high O_2 states is effectively impossible at 1000 ppmv CH_4, but is relatively easy for $f(CH_4) < 10$ ppmv. These are high volcanic SO_2 flux models (V3).

seasonal timescales, O_2 production and consumption are out of balance by 4×10^{12} cm^{-2} s^{-1}, which is on the order of 10% of the total production.

Before O_2 became plentiful, respiration would have been local, confined to oxygen oases in the immediate vicinity of the photosynthetic source, and probably diurnal. Thus, there is no reason to expect that respiration should so nearly cancel O_2 emission as it does today, and we might reasonably expect the flux of O_2 into the atmosphere to have been as large as the annual imbalance today.

For specificity we have set an upper bound on the O_2 flux into the atmosphere at 1×10^{13} cm^{-2} s^{-1}. This is 25% of the modern total photosynthetic production, and 2.5 times bigger than today's net production/respiration imbalance on a seasonal timescale. We have set the lower bound at 1×10^{11} cm^{-2} s^{-1}. This is 2.5 times the modern net O_2 flux averaged over geological time scales. The lower bound is very conservative, given how rapidly O_2 would be consumed either in the environment by oxidative weathering or in the atmosphere by photochemistry (cf. Walker, 1987). For comparison Pavlov & Kasting (2002) set higher upper and lower bounds of $6 \times 10^{11} < \phi(O_2) < 3 \times 10^{13}$ cm^{-2} s^{-1}.

Figure 6 is analogous to Fig. 5 for a range of methane mixing ratios. To limit clutter only the O_2 flux, the H escape, and the S_8 fallout are shown. Methane mixing ratios range from 1 to 1000 ppmv. Not surprisingly, the more methane-rich atmospheres are more reduced and permit proportionately higher levels of hydrogen escape. At $f(CH_4) < 10^{-3}$ only highly anoxic atmospheres (featuring $f(O_2) < 10^{-8}$) are accessible with $\phi(O_2) < 10^{13}$ cm^{-2} s^{-1}. The model predicts that such atmospheres generate S_8 abundantly. By contrast, we regard any $f(O_2)$ level as potentially accessible for CH_4 mixing ratios smaller than 30 ppmv.

Ono *et al.* (2003) showed that sulfur speciation depended on the methane mixing ratio, with the more strongly reduced atmospheres making more strongly reduced sulfur. One difference between our results and those reported by Ono *et al.* (2003) is that our reduced models are significantly less reduced than theirs. In their most reduced atmospheres, Ono *et al.* (2003) predicted that rainout or surface deposition of H_2S and the radical HS represent important atmospheric exit channels. We do not see this, and we have no explanation for the different model behaviours.

Figure 7 shows that S_8 production is a strong function of methane mixing ratio for the high modern volcanic SO_2 flux (Case V2) and for a ground-level oxygen mixing ratio $f(O_2) = 10^{-7}$. Higher $f(O_2)$ shifts the S_8 cutoff to higher $f(CH_4)$, and lower $f(O_2)$ shifts the S_8 cutoff to lower $f(CH_4)$. A similar figure was presented by Ono *et al.* (2003; their Fig. 4) for extremely anoxic atmospheres with no biogenic O_2 source. In the absence of O_2 the dependence of S_8 production on $f(CH_4)$ is not as strong.

Ono *et al.* (2003) also showed that S_8 production is a strong function of the volcanic SO_2 source. They considered three SO_2 fluxes, two of which were equivalent to our V2 and V1 models, and a third with a smaller SO_2 flux of 3.5×10^8 cm^{-2} s^{-1}. They found that S_8 production is shut off at low SO_2 fluxes and low levels of CH_4. We see much the same.

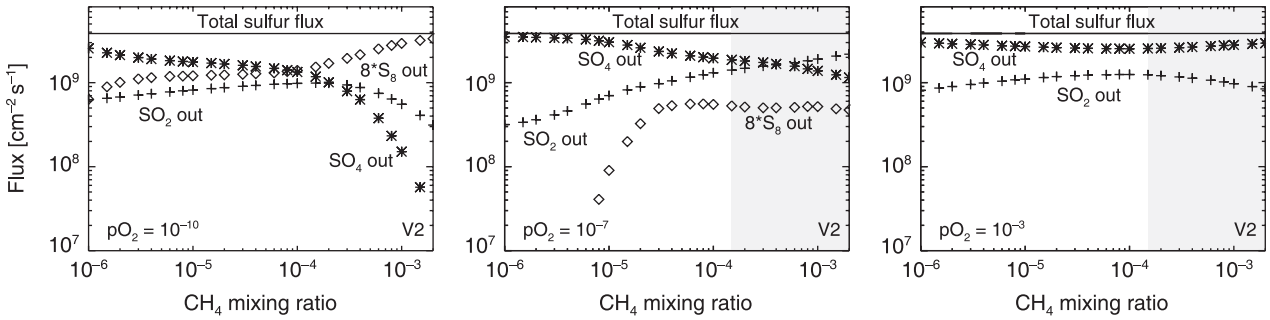

Fig. 7 Sulfur fluxes as a function of CH_4 mixing ratio at a ground-level O_2 mixing ratio of 10^{-7}. In this particular example, with $f(O_2)$ fixed, S_8 production, and by presumption MIF S, shuts off for $f(CH_4) < 8$ ppmv. Volcanic fluxes are at the high modern levels (V2).

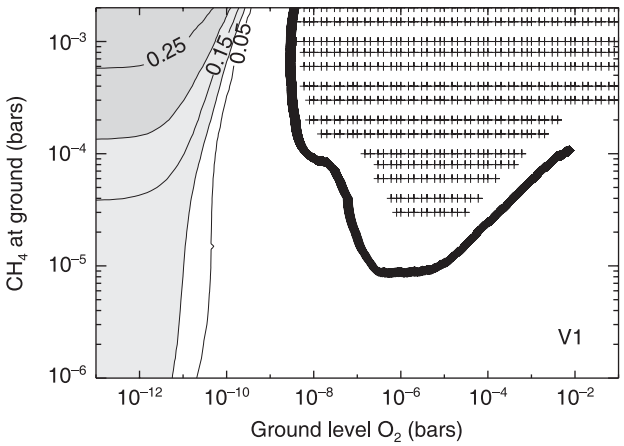

Fig. 8 S_8 production in Tmol-S year^{-1} plotted on a grid of ground-level O_2 and CH_4 mixing ratios. This is for our low modern volcanic flux case V1. Atmospheres that require net O_2 fluxes greater than 1×10^{13} cm^{-2} s^{-1} are marked with '+' symbols. For reasons described in the text, we regard these as inaccessible. Significant S_8 production is limited to atmospheres with ground-level $f(O_2) < 2 \times 10^{-10}$. In these models ground-level $f(O_2) < f(CH_4)$ are effectively proxies for $\phi(O_2)$. We argue in the text that $\phi(O_2)$ is unlikely to be small enough to allow $f(O_2) < 10^{-10}$. We therefore do not expect MIF S for volcanic S fluxes as small as the fluxes in V1. Also shown on the plot is the trajectory of Claire *et al.*'s (2006) reference model. The Claire *et al*. (2006) model evolves in a counter-clockwise sense along this curve. For V1 fluxes the Claire *et al*. reference model never generates MIF S.

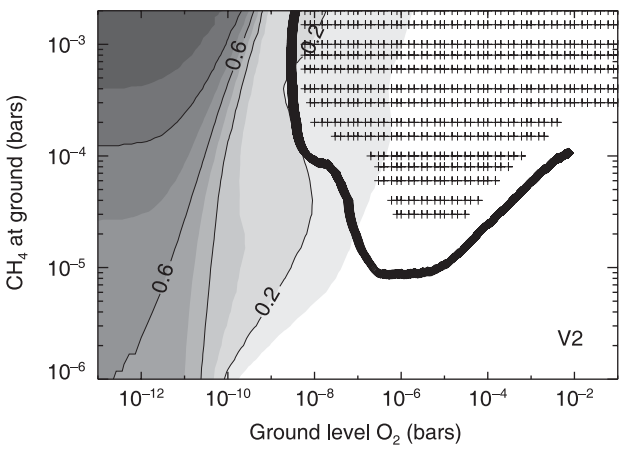

Fig. 9 S_8 production in Tmol-S year^{-1} plotted on a grid of ground-level O_2 and CH_4 mixing ratios for our high modern volcanic flux case V2. The Claire *et al*. (2006) reference model provides a credible history in this case. This history is replotted on Fig. 12 below.

Figures 8, 9, and 10 are contour plots that show the computed S_8 production as a function of $f(O_2)$ and $f(CH_4)$. These figures indicate the range of atmospheres that can give rise to substantial S_8 production. Production is given in units of Tmol of S per annum.

Figure 8 addresses our low modern volcanic flux (V1) models with $\phi(SO_2) = 1 \times 10^9$ cm^{-2} s^{-1} and $\phi(H_2S) = 1 \times 10^8$ cm^{-2} s^{-1}.

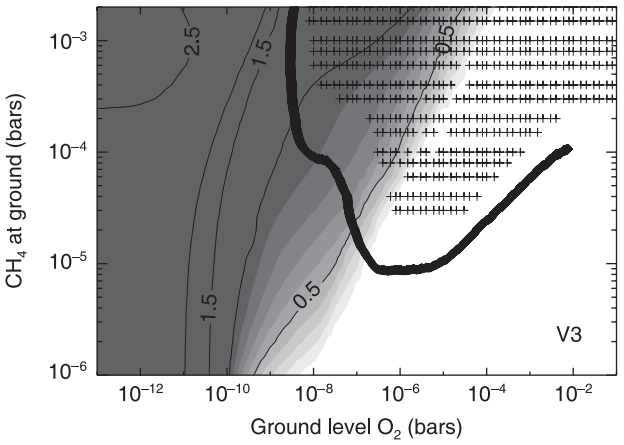

Fig. 10 S_8 production in Tmol-S year^{-1} plotted on a grid of ground-level O_2 and CH_4 mixing ratios for our high Archean volcanic flux case V3. It is noteworthy that the threshold for S_8 production is as strong a function of $f(CH_4)$ as it is of $f(O_2)$ at the higher S fluxes. The Claire *et al*. (2006) reference model also fares well in this case.

Atmospheres that require net O_2 fluxes greater than 1×10^{13} cm^{-2} s^{-1} are marked. For reasons discussed above, we regard O_2 fluxes greater than 1×10^{13} cm^{-2} s^{-1} as implausible. With this limitation, ground-level O_2 mixing ratios $2 \times 10^{-7} < f(O_2) < 2 \times 10^{-4}$ are inaccessible for $f(CH_4) \geq 5 \times 10^{-5}$. By net fluxes, we refer to the difference between production and respiration on timescale longer than the characteristic response time of the atmosphere. For an anoxic atmosphere with $f(O_2) < 10^{-7}$, the lifetime of atmospheric O_2 is measured in days to weeks. It seems obvious that such an atmosphere would be strongly driven by variable biogenic fluxes, so that specific steady state solutions such as those discussed here have limited value. For oxic solutions with $f(O_2) > 10^{-4}$, the O_2 lifetimes range from a decade up.

For the low SO_2 flux (Fig. 8), significant S_8 production is limited to atmospheres with ground-level $f(O_2) < 10^{-10}$. To first approximation very low $f(O_2)$ is better regarded as a proxy for $\phi(O_2)$ than as an actual O_2 mixing ratio. This occurs because the troposphere is both very reduced and very photochemically active. For all the models considered in this study, for very low $f(O_2) \sim 10^{-10}$ the relation between the flux and the mixing ratio is nearly linear and approximately given by $\phi(O_2) \approx 5 \times 10^{20} f(O_2)$ cm^{-2} s^{-1} (Fig. 6). If we take $\phi(O_2) > 10^{11}$ cm^{-2} s^{-1}, we would conclude that S_8 and therefore strong MIF S is unlikely for SO_2 fluxes smaller than 1×10^9 cm^{-2} s^{-1}.

Figure 9 addresses our high modern volcanic flux (V2) models with $\phi(SO_2) = 3.5 \times 10^9$ cm^{-2} s^{-1} and $\phi(H_2S) = 3.5 \times 10^8$ cm^{-2} s^{-1}. The inaccessible regions do not change appreciably for the different volcanic fluxes. Higher S fluxes increase the stability field of S_8. Dependence of S_8 production on $f(CH_4)$ is more pronounced than for smaller volcanic fluxes.

Figure 10 addresses our high Archean volcanic flux (V3) models with $\phi(SO_2) = 1 \times 10^{10}$ cm^{-2} s^{-1} and $\phi(H_2S) = 1 \times$

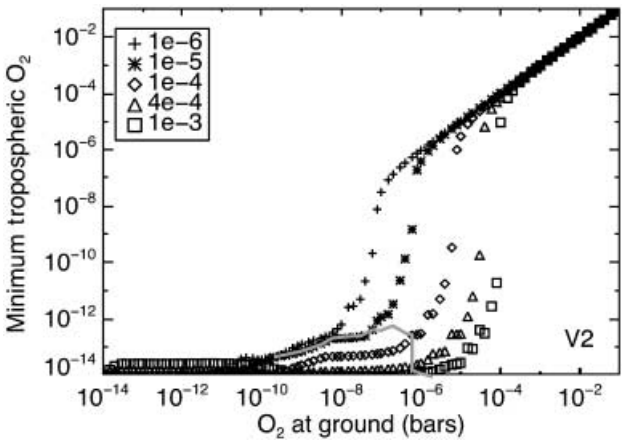

Fig. 11 The minimum tropospheric oxygen levels ($f(O_2)$) as a function of the ground-level oxygen mixing ratio ($f_{gr}(O_2)$), labelled by the methane mixing ratio ($f(CH_4)$). For low O_2 and high CH_4 the troposphere are highly anoxic. At high O_2 ground-level mixing ratios the oxygen becomes well-mixed, as indicated by the diagonal line ($f_{tr}(O_2) \approx f_{gr}(O_2)$) rising to the right. The transition is abrupt, especially at the higher methane levels for which oxic atmospheres are in any event impossible. The snaking solid grey curve represents the threshold for S_8 production. S_8 production is always confined to atmospheres that feature extremely anoxic tropospheres. It is noteworthy that the atmosphere can be very anoxic and yet not generate S_8, even at, or especially at, high methane levels. The ground-level mixing ratio $f_{gr}(O_2) \approx 10^{-6}$ for high $f(CH_4)$ is essentially the same result obtained by Pavlov & Kasting (2002) for the equivalent case. These computations use volcanic flux model V2.

10^9 cm^{-2} s^{-1}. At the higher S fluxes, S_8 production – especially the threshold for S_8 production, which may be the key quantity of interest – is as strong a function of $f(CH_4)$ as it is of $f(O_2)$.

As a general rule all of the atmospheres that generate significant S_8 are quite anoxic. In particular the tropospheres are very anoxic except near the ground. This point is made more clearly in Fig. 11, which shows S_8 production vs. the minimum $f(O_2)$ in the troposphere for the high modern volcanic fluxes (Case V2). These are the same models shown in Fig. 9. For the more reduced atmospheres the ground-level O_2 mixing ratio is better understood as a proxy for the biogenic flux into the atmosphere. Instead of a small constant ground-level mixing ratio, one should imagine localized O_2-rich plumes emitted from photosynthetically active regions, mixing into and chemically reacting with the ambient tropospheric gases.

DISCUSSION

The steadily widening envelope of mass-*dependent* sulfur fractionation (a.k.a. $\delta^{34}S$) seen through the Archean and early Proterozoic has been interpreted as a history of sulfate availability (Canfield, 2005). In the early Archean, mass dependent S fractionation is modest. Evidently, S was in short supply and at most times in most places all of it was used up. Hence the natural inclination of biology to discriminate between the heavy and light isotopes of sulfur was not expressed: if every atom of sulfur is used, there is no fractionation. To first approximation we might regard the sulfate fractionation that did not occur as a measure of the organic matter left over after the sulfate was consumed. It is well known that sulfate reducers outcompete methanogens; when sulfate is abundant methanogenesis is suppressed, but when the sulfate is gone away, the methanogens can play. The organic leftovers provided the substrate for the methanogens. The suppression of mass-dependent S fractionation through the Archean implies that methanogens ate well, and that methane fluxes into the atmosphere were big.

The envelope of $\delta^{34}S$ appears to increase steadily through the late Archean and through the early Proterozoic, reaching modern levels ca. 1.8–2.0 Ga. The increasing span of $\delta^{34}S$-values implies that as time passed biology was being afforded more opportunities to discriminate between sulfur's isotopes. Evidently it was becoming more common to exhaust the pool of available organic matter before exhausting the pool of available sulfur. With less organic matter escaping sulfate reduction, there would be less organic matter reduced to methane and therefore a smaller source of methane. This also implies that the pool of available sulfur was growing. These seem to have been long-term trends that continued well into the Proterozoic. These trends imply a steady decline in the relative importance of methanogens.

As sulfate reducers gained prominence, it is likely that biogenic S-containing gases became more important. As noted above, biogenic sulfur gases include H_2S, DMS, OCS, and CS_2. It is possible that they achieved a level of importance in the anoxic late Archean or early Proterozoic atmosphere that they have not risen to since. The sulfur gases are much more photochemically reactive than methane; indeed, they are more reactive than O_2. At this point the role of biogenic sulfur gases is entirely speculative, but it is clear that to the extent they replaced CH_4 or H_2 as the reduced partner of photosynthetic O_2 they worked to favour the creation of an O_2 atmosphere.

The story told in this paper begins with the invention of oxygenic photosynthesis. A likely consequence of this invention was a general increase in global productivity. Another likely consequence was an increase in atmospheric methane, because methane is a biological end-product and it is chemically more stable than O_2. Because methane is a potent greenhouse gas, it warmed the Earth. The warmer conditions promoted CO_2-consuming weathering reactions, which suggests that atmospheric CO_2 levels were probably reduced by the increased methane.

A key consequence of abundant atmospheric methane was nontrivial H escape to space. Hydrogen escape irreversibly oxidizes the Earth, especially the near surface reservoirs, and the crust in particular (Catling *et al.*, 2001). It takes hundreds of millions of years to oxidize key crustal reservoirs of iron and sulfur. Both iron and sulfur record this history in their fractionated isotopes. With sulfur the record seems straightforward:

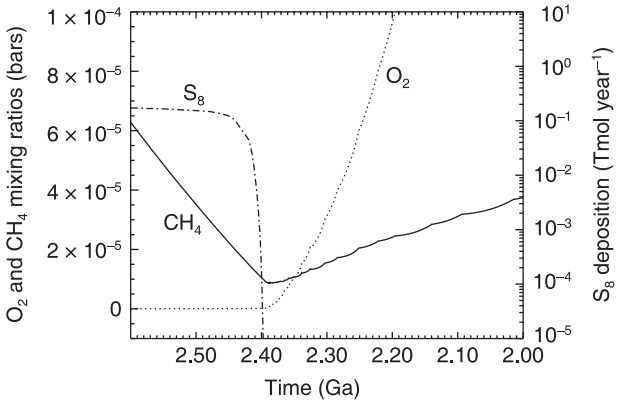

Fig. 12 Histories of $f(CH_4)$, $f(O_2)$, and S_8 production as the atmosphere evolves along the trajectory defined by Claire *et al.*'s (2006) reference model. The order of events given here is general to any plausible narrative of the oxic transition. First MIF S disappears, then CH_4 reaches a minimum and temperatures reach a minimum because of this, then O_2 rises to mildly oxic levels, and finally CH_4 returns to provide greenhouse warming under the protection of an oxygen-ozone shield.

available oceanic sulfate steadily increased through the Archean, as one expects of an inexorably oxidized crust.

As the oceanic sulfate pool increased, greater competition with sulfate reducers left less room for methanogens. Net methane production must have decreased and atmospheric methane levels must have decreased accordingly (the O_2 flux to the atmosphere would also have decreased, although $\phi(O_2)$'s decrease may have been offset somewhat by increased emission of photochemically labile biogenic S-gases and of biogenic H_2). The decline of CH_4 caused sulfur MIF to stop and the climate to cool, the latter culminating in severe ice ages. This sequence of events is nicely illustrated in Fig. 12, which creates a history of MIF S by combining Claire *et al.*'s (2006) reference model for the histories of atmospheric O_2 and CH_4 with the S_8 production rates shown in Fig. 9. The order of events is general: (i) oceanic sulfate increases, (ii) atmospheric methane declines, (iii) sulfur MIF disappears and greenhouse warming collapses, (iv) oxygen rises and the methane greenhouse returns under the photochemical protection of abundant oxygen and ozone.

We speculate that it was the increasing sulfate pool and the concomitant reduction of atmospheric methane that made the transition to an oxic atmosphere possible. While CH_4 and O_2 fluxes remained large and methane abundant the atmosphere remained trapped in a stable anoxic state, as we showed most clearly in connection with Fig. 5. Although oxic atmospheres exist with essentially the same biogenic forcings as those driving the anoxic atmosphere, the oxic states are inaccessible when methane is abundant in the atmosphere. This is seen in Figs 5, 6, and 8–10. At lower levels of atmospheric CH_4 the barrier against transition to an O_2-rich atmosphere is small enough that realistic biogenic fluxes can overcome it. It is no accident that the rise of O_2 took place during ice ages at a time when atmospheric CH_4 levels were low.

CONCLUSIONS

- We assumed that the characteristic of the Archean sulfur MIF signal is a product of atmospheric photochemistry, and that the photochemical signature was preserved in the rock record when sulfur was able to leave the atmosphere in both soluble (e.g. SO_2, H_2SO_4) and insoluble (S_8) forms. We used a 1-D atmospheric photochemistry model to characterize the conditions conducive to the condensation and precipitation of particles of elemental sulfur. We assumed a volcanic source of sulfur gases. Our models presume oxygenic photosynthesis and a rough stochiometric balance between the net fluxes of O_2 and CH_4 into the atmosphere.
- Precipitation of S_8 depends on the SO_2 source and the mixing ratios of CH_4 and O_2. In particular, we showed that S_8 deposition is a strong function of CH_4 for oxygen levels and SO_2 sources likely in the late Archean. The necessary conditions for forming S_8 are best understood as requiring a large sulfur source, an anoxic troposphere, and a sufficient amount of a reduced gas (either CH_4 or H_2 will do). All three requirements must be met to form S_8.
- Collapse of atmospheric methane in the late Archean to below 10 ppmv provides the best explanation of the disappearance of MIF in sulfur. This differs from previous work attributing the loss of MIF to the rise of O_2. We suggest that the methane collapse was driven by the increasing importance of sulfate and the increasing competitive advantage of sulfate reducers over methanogens. The collapse of CH_4 also explains widespread low-latitude glaciation in the early Proterozoic.
- We suggest that the growth of the oceanic sulfate pool reflects secular changes in the redox balance of the atmosphere–ocean–crust system, probably driven by hydrogen escape.
- The rise of O_2 to geologically detectable levels took place after the collapse of MIF, and was facilitated by generally low levels of atmospheric methane characteristic of the ice ages.
- The ice ages were ended by the rise of O_2. The Proterozoic was relatively rich in methane (at ~100 ppmv levels) because the ozone layer provided methane with protection against photochemical destruction.

ACKNOWLEDGEMENTS

We thank Jim Kasting, Euan Nisbet, and an anonymous reviewer for helpful discussions regarding this work; we also thank Jim Kasting for giving us his sulfur photochemistry code many years ago. For this work, K. Zahnle was supported by NASA's Exobiology Program and Astrobiology Institute. M. Claire was supported by a NASA Graduate Student Research Fellowship. D. Catling was supported by Exobiology Program

grant NNG05GQ25G awarded to the University of Washington. D. Catling also acknowledges support from a European Union Marie Curie Chair award at the University of Bristol.

REFERENCES

Aiuppa A, Inguaggiato S, McGonigle AJS, O'Dwyer M, Oppenheimer C, Padgett MJ, Rouwet D, Valenza M (2005) H_2S fluxes from Mt. Etna, Stromboli, and Vulcano (Italy) and implications for the sulfur budget at volcanoes. *Geochimica et Cosmochimica Acta* **69**, 1861–1871.

Andres RJ, Kasgnoc AD (1998) A time-averaged inventory of subaerial volcanic sulfur emissions. *Journal of Geophysical Research-Atmospheres* **103**, 25251–25261.

Arthur MA (2000) Volcanic contributions to the carbon and sulfur geochemical cycles and global change. In *Encyclopedia of Volcanoes* (ed. Sigurdsson H). Academic Press, pp. 1045–1056.

Bekker A, Holland HD, Wang PL, Rumble D, Stein HJ, Hannah JL, Coetzee LL, Beukes NJ (2004) Dating the rise of atmospheric oxygen. *Nature* **427**, 117–120.

Brocks JJ, Logan GA, Buick R, Summons RE (1999) Archean molecular fossils and the early rise of eukaryotes. *Science* **285**, 1033–1036.

Brocks JJ, Buick R, Summons RE, Logan GA (2003) A reconstruction of Archean biological diversity based on molecular fossils from the 2.78 to 2.45 billion-year-old Mount Bruce Supergroup, Hamersley Basin, Western Australia. *Geochimica et Cosmochimica Acta* **67**, 4321–4335.

Canfield DE (2005) The early history of atmospheric oxygen: homage to Robert M. Garrels. *Annual Reviews of Earth and Planetary Science* **33**, 1–36.

Canfield DE, Habicht KS, Thamdrup B (2000) The Archean sulfur cycle and the early history of atmospheric oxygen. *Nature* **288**, 658–661.

Catling DC (2006) Comment on 'A Hydrogen-Rich Early Earth Atmosphere'. *Science* **311**, 38a–.

Catling DC, Claire MW (2005) How Earth's atmosphere evolved to an oxic state: A status report. *Earth and Planetary Science Letters* **237**, 1–20.

Catling DC, Zahnle KJ, McKay CP (2001) Biogenic methane, hydrogen escape, and the irreversible oxidation of early Earth. *Science* **293**, 839–843.

Charlson RJ, Lovelock JE, Andreae MO, Warren SG (1987) Oceanic phytoplankton, atmospheric sulphur, cloud albedo and climate. *Nature* **326**, 655–661.

Claire MW, Catling DC, Zahnle KJ (2006) Biogeochemical modeling of the rise in atmospheric oxygen. *Geobiology*, Doi: 10.1111/j.1472-4669.2006.00084.x.

Cloud P (1968) Atmospheric and hydrospheric evolution on the primitive Earth. *Science* **160**, 729–736.

Cloud P (1988) *Oasis in Space*. Norton, New York, pp. 509.

Des Marais DJ, Strauss H, Summons RE, Hayes JM (1992) Carbon isotope evidence for the stepwise oxidation of the Proterozoic environment. *Nature* **359**, 605–609.

Farquhar J, Wing BA (2003) Multiple sulfur isotopes and the evolution of the atmosphere. *Earth and Planetary Science Letters* **213**, 1–13.

Farquhar J, Wing BA (2005) The terrestrial record of stable sulphur isotopes: a review of the implications for evolution of Earth's sulphur cycle. In *Mineral Deposits and Earth Evolution* (eds McDonald I, Boyce AJ, Butler IB, Herrington RJ, Polya DA). Geological Society, Special Publications, London, 248, 167–177.

Farquhar J, Bao H, Thiemans M (2000) Atmospheric influence of Earth's earliest sulfur cycle. *Science* **289**, 756–758.

Farquhar J, Savarino J, Airieau S, Thiemens MH (2001) Observation of wavelength-sensitive mass-independent sulfur isotope effects during SO_2 photolysis: application to the early atmosphere. *Journal of Geophysics Research* **106**, 1–11.

Hoehler TM, Bebout BM, DesMarais DJ (2001) The role of microbial mats in the production of reduced gases on the early Earth. *Nature* **412**, 324–327.

Holland HD (1984) *The Chemical Evolution of the Atmosphere and Oceans*. Princeton University Press, Princeton, pp. 582.

Holland HD (2002) Volcanic gases, black smokers, and the Great Oxidation Event. *Geochimica et Cosmochimica Acta* **66**, 3811–3826.

Karhu JA, Holland HD (1996) Carbon isotopes and the rise of atmospheric oxygen. *Geology* **24**, 867–870.

Kasting JF (1990) Bolide impacts and the oxidation state of carbon in the Earth's early atmosphere. *Origins of Life and Evolution of the Biosphere* **20**, 199–231.

Kasting JF (1993) Earth's early atmosphere. *Science* **259**, 920–926.

Kasting JF, Zahnle KJ, Pinto JP, Young AT (1989) Sulfur, ultraviolet radiation, and the early evolution of life. *Origins of Life* **19**, 95–108.

Kharecha P, Kasting JF, Siefert J (2005) A coupled atmosphere-ecosystem model of the early Archean Earth. *Geobiology* **3**, 53–76.

Kopp RE, Kirschvink JL, Hilburn IA, Nash CZ (2005) The Paleoproterozoic snowball Earth: a climate disaster triggered by the evolution of oxygenic photosynthesis. *Proceedings of the National Academy of Sciences of the USA* **102**, 11131–11136.

Manabe S, Wetherald RT (1967) Thermal equilibrium of the atmosphere with a given distribution of relative humidity. *Journal of Atmospheric Sciences* **24**, 241–259.

Marty B, Tolstikhin IN (1998) CO_2 fluxes from mid-ocean ridges, arcs and plumes. *Chemical Geology* **145**, 233–248.

Masterson AL, Wing BA, Farquhar JA, Franz H, Lyons JR (2006) Poster 226 – Anomalous isotopic fractionation during broadband SO_2 photochemistry: contributions from direct and indirect photodissociation. *Astrobiology* **6**, p. 192.

Ono S, Eigenbrode JL, Pavlov AA, Kharecha P, Rumble D III, Kasting JF, Freeman KH (2003) New insights into Archean sulfur cycle from mass-independent sulfur isotope records from the Hamersley Basin, Australia. *Earth and Planetary Science Letters* **213**, 15–30.

Papineau D, Mojzsis SJ, Coath CD, Karhu JA, McKeegan KD (2005) Multiple sulfur isotopes of sulfides from sediments in the aftermath of Paleoproterozoic glaciations. *Geochimica et Cosmochimica Acta* **69**, 5033–5060.

Pavlov AA, Kasting JF (2002) Mass-independent fractionation of sulfur isotopes in Archean sediments: strong evidence for an anoxic Archean atmosphere. *Astrobiology* **2**, 27–41.

Pavlov AA, Kasting JF, Brown LL (2001) UV-shielding of NH_3 and O_2 by organic hazes in the Archean atmosphere. *Journal of Geophysical Research* **106**, 23267–23287.

Pavlov AA, Kasting JF, Brown LL, Rages KA, Freedman R (2000) Greenhouse warming by CH_4 in the atmosphere of early Earth. *Journal of Geophysical Research* **105**, 11981–11990.

Ribas I, Guinan EF, Gudel M, Audard M (2005) Evolution of the solar activity over time and effects on planetary atmospheres. I. High-energy irradiances (1–1700 angstrom). *Astrophysical Journal* **622**, 680–694.

Rye R, Kuo PH, Holland HD (1995) Atmospheric carbon dioxide concentrations before 2.2 billion years ago. *Nature* **378**, 603–605.

Savarino J, Romero A, Cole-Dai J, Bekki S, Thiemens M (2003) UV induced mass-independent sulfur isotope fractionation in stratospheric volcanic sulfate. *Geophysical Research Letters* **30**, Cite ID 2131.

Sleep NH, Bird DK (2007) Niches of the pre-photosynthetic

biosphere and geologic preservation of Earth's earliest ecology. *Geobiology*, in press.

Sleep NH, Zahnle KJ (2001) Carbon dioxide cycling and implications for climate on ancient Earth. *Journal of Geophysical Research* **106**, 1373–1399.

Summons RE, Bradley AS, Jahnke LL, Waldbauer JR (2006) Steroids, triterpenoids and molecular oxygen. *Philosophical Transactions of the Royal Society of London. Series B-Biological Sciences* **361**, 951–968.

Tian F, Toon OB, Pavlov AA, De Sterck H (2005) A hydrogen-rich early Earth atmosphere. *Science* **308**, 1014–1017.

Toon OB, Kasting JF, Turco RP, Liu MS (1987) The sulfur cycle in the marine atmosphere. *Journal of Geophysical Research* **92**, 943–963.

Valentine DL (2002) Biogeochemistry and microbial ecology of methane oxidation in anoxic environments: a review. *Antonie Van Leeuwenhoek* **81**, 271–282.

Walker JCG (1977) *Evolution of the Atmosphere*. Macmillan, New York.

Walker JCG (1987) Was the Archaean biosphere upside-down? *Nature* **329**, 710–712.

Walker JCG, Brimblecombe P (1985) Iron and sulfur in the pre-biologic ocean. *Precambrian Research* **28**, 205–222.

Walker JCG, Klein C, Schidlowski M, Schopf JW, Stevenson DJ, Walter MR (1983) Environmental evolution of the Archean–Early Proterozoic Earth. In *Earth's Earliest Biosphere* (ed. Schopf JW). Princeton University Press, Princeton, New Jersey, pp. 260–290.

Zahnle KJ (1986) Photochemistry of methane and the formation of hydrocyanic acid (HCN) in the Earth's early atmosphere. *Journal of Geophysical Research* **91**, 2819–2834.

Zahnle KJ, Sleep NH (2002) Carbon dioxide cycling through the mantle and implications for the climate of ancient Earth. In *The Early Earth: Physical Chemical and Biological Development* (eds Fowler CM, Ebinger CJ, Hawkesworth CJ). Geological Society of London Special Publication, 199. Geological Society of London, London, UK, pp. 231–257.